Jurnal Rekayasa Mesin
p-ISSN: 1411-6863, e-ISSN: 2540-7678
Vol.20, No.3, December **2025**, p. 351-358

Corrosion Behavior of Al6061-T6 by GTAW with Different Filler Metals

Suherman[1*], Muharnif[1], Riadini Wanty Lubis[1], Irfansyah[1] and F.X.A Wahyudianto[2]
[1]Department of Mechanical Engineering, Universitas Muhammadiyah Sumatera Utara-Indonesia
Jl. Kapt. Mukhtar Basri No. 3 Medan, 20238, Sumatera Utara, Indonesia
[2]Department of Mechanical Engineering, Politeknik Negeri Samarinda-Samarinda-Indonesia
[2]Jl. Cipto Mangunkusumo, Kampus Gunung Lipan, Sungai Keledang, Kota Samarinda, Kalimantan Timur, Indonesia
*E-mail: suherman@umsu.ac.id

Submitted: 23-05-2025; Accepted: 02-12-2025; Published: 30-12-2025

Abstract

This study aims to compare the effect of filler metal of gas tungsten arc welding (GTAW) on the corrosion rate of Al6061 alloy weld metals. Three different filler metals, ER4043, ER4047, and ER5356, were used in the GTAW welding process. The corrosion rate characteristics of butt weld joints were studied using potentiodynamic testing in a 3.5% NaCl solution. The microstructure of the corroded weld metal was analyzed using Scanning Electron Microscopy (SEM). Results showed that filler metals affect the corrosion resistance of weld metal. It was found that ER4043 and ER4047 are more susceptible to corrosion, while ER5356 shows good corrosion resistance compared to the other filler metals. SEM observations revealed that dominant pitting corrosion was found in all welded joints and the base metal, with pit diameters ranging from 10 to 60 μm. Moreover, it was found that the Heat-Affected Zone was more susceptible to corrosion compared to the weld metal zone. Finally, welding of Al6061 using ER5356 filler metal is more recommended due to its superior resistance to pitting corrosion compared to the other types of joints.

Keywords: *Al6061; corrosion; ER4043; ER4047; ER5356*

Abstrak

Studi ini bertujuan untuk membandingkan pengaruh logam pengisi dalam proses pengelasan Gas Tungsten Arc Welding (GTAW) terhadap laju korosi logam las paduan Al6061. Tiga jenis logam pengisi yang berbeda, yaitu ER4043, ER4047, dan ER5356, digunakan dalam proses pengelasan GTAW. Karakteristik laju korosi dari sambungan las butt diteliti menggunakan pengujian potensiodinamik dalam larutan NaCl 3,5%. Mikrostruktur logam las yang telah mengalami korosi dianalisis menggunakan Scanning Electron Microscopy (SEM). Hasil menunjukkan bahwa logam pengisi memengaruhi ketahanan korosi dari logam las. Ditemukan bahwa ER4043 dan ER4047 lebih rentan terhadap korosi, sedangkan ER5356 menunjukkan ketahanan korosi yang baik dibandingkan dengan logam pengisi lainnya. Pengamatan SEM menunjukkan bahwa korosi pitting yang dominan ditemukan pada semua sambungan las dan logam dasar, dengan diameter pit berkisar antara 10 hingga 60 μm. Selain itu, ditemukan bahwa daerah Heat-Affected Zone (HAZ) menunjukkan lebih rentan terhadap serangan korosi dibandingkan dengan zona logam las. Akhirnya, pengelasan Al6061 menggunakan logam pengisi ER5356 lebih direkomendasikan karena ketahanannya yang unggul terhadap korosi pitting dibandingkan dengan jenis sambungan lainnya.

Kata kunci: *Al6061; corrosion; ER4043; ER4047; ER5356*

1. Introduction

Aluminum 6061 is extensively utilized due to its excellent workability, weldability, and resistance to corrosion [1]. AA6061 is primarily composed of magnesium and silicon, and it is commonly strengthened through precipitation hardening [2]. Aluminum alloys are widely used in various applications, such as in the aerospace and defense sectors [3], structures, wind and solar energy [4], rocket fuel tanks and ammunition [5], automotive, transportation, and aircraft frames. Aluminum is generally known as a lightweight material with good corrosion resistance [3], excellent conductivity, and environmentally friendly properties [3, 6]. Aluminum alloys have a high strength-to-density ratio [7].

Corrosion poses a significant issue, especially in welded joints exposed to corrosive environments like seawater. The Al_2O_3 protective layer on the surface is essential in preventing severe oxidation of the underlying alloy [8]. Although this protective mechanism exists, AA6xxx alloys remain vulnerable to localized corrosion in harsh

environments, mainly due to the presence of Fe-rich intermetallic compounds and Mg_2Si [9]. Research on the corrosion rate of welded aluminum alloys has been extensively studied. Weld joints of Al6061 using the GTAW method exhibit lower corrosion resistance compared to FSW joints [10]. Furthermore, Priyasudana, et al. [11] stated that FSW welding with a 1G welding position has the highest corrosion rate compared to others. In GTAW welding, the HAZ (heat-affected zone) is the most susceptible area to corrosion [12]. Yang and Huang [13] also reported that the corrosion resistance of weld joints is greater than that of the base metal experiencing pitting corrosion. The artificial aging process on aluminum alloys tends to provide more uniform corrosion resistance. The aging process also reduces the tendency for intergranular corrosion, while pitting corrosion occurs in the HAZ and base metal. This type of corrosion shifts from pitting and intergranular corrosion to primarily pitting corrosion [14]. A review of corrosion testing on Al6061 using various corrosion methods is presented in Table 1.

In this study, Al6061 aluminum alloy was welded using the Gas Tungsten Arc Welding (GTAW) method with different filler metals (ER4043, ER4047, and ER5356. The Corrosion rate tests were conducted to determine the corrosion characteristics of the weld joints using Potentiodynamic polarization (PD) tests. The corroded surface of each specimen was examined using SEM (Scanning Electron Microscopy).

Table 1. Overview of corrosion test of Aluminium alloys

Materials	Welding Methods	Filler Metals	Corrosion methods	Solution	Result	Ref
Al6061	GTAW	ER4043	electroetching electric potential	3.5 wt. % NaCl	Corrosion rate FSW < GTAW	[10]
Al6061	GMAW	ER4043, ER5356, FMg0.6	potentiodynamic polarization test	3.5 wt. % NaCl	Corrosion rate FMg0.6>ER4043>ER5356	[9]
Al6061	Friction Welded	-	three-electrode cell potentiostat	3.5 wt. % NaCl	Specimen B with the 1G position has the highest corrosion rate of 0.63856 mm/year.	[11]
Al6061	Friction Welded	-	Potentiostat controlled by softcorr 352	NaCl	Intergranular corrosion and pitting corrosion	[15]
Al6061	Friction Welded		potentiodynamic polarization test	3.5 wt. % NaCl	Weld metal higher susceptibility to pitting corrosion and stress corrosion cracking compared to the base metal	[16]
AA2014	GTAW	-	potentiodynamic polarization test	3.5 wt. % NaCl	Corrosion rate FSW > GTAW	[12]
ADC12	GTAW	ER4043	CS350 electrochemical workstation	3.5 wt. % NaCl	uniformly corroded	[13]
Al2024	friction welded	-	electrochemical workstation CS310H	3.5 wt. % NaCl	corrosion resistance of BM>TMAZ> HAZ > DRZ	[14]

2. Material and Method

2.1 Materials

The materials employed in this study consisted of 4 mm-thick Al6061 alloy plates, joined using ER4043, ER4047, and ER5356 filler metals. The chemical compositions of these materials are presented in Table 1. The solutions: 3.5% sodium chloride (NaCl) with a pH of 6.8.

Table 2. Chemical composition (wt%)

Materials	Si	Fe	Cu	Mn	Mg	Cr	Zn	Ti
Al6061	0.48	0.27	0.18	0.05	0.92	0.09	0.03	0.06
ER4043	4.124	0.431	0.2	0.002	0.006	0.008	0.011	0.018
ER4047	11.2	0.08	0.3	0.15	1.1	-	0.2	-
ER5356	0.25	0.4	0.1	0.5	4.8	0.19	0.10	0.11

2.2 Methode

The surfaces of the coupons were polished using abrasive paper to eliminate the oxide layer. In this study, aluminium plate welding was performed employing GTAW (Type 250 AC/DC) and GMAW (AUTOMIG Type 273) welding machines (Migatronic A/S 9690, Denmark). The welding parameters applied included a current of 12.5 V, a travel speed of 5.2 mm/s, an alternating current of 140 A, and a gas flow rate of 15 l/min. The filler metal used had a diameter of 2.6 mm [17] .

a. Samples Preparation

The coupon is then cut to prepare corrosion test specimens, as shown in Figure 1. The test specimens are subsequently polished using sandpaper grit 800.

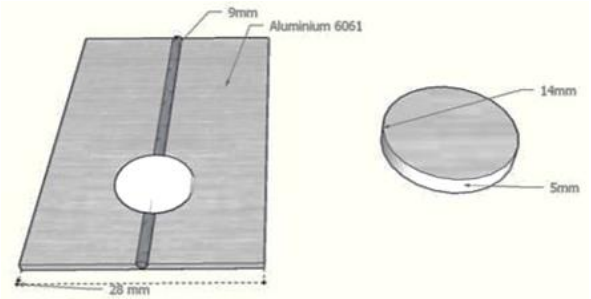

Figure 1. Coupon for corrosion test specimens.

b. Electrochemical Test

Electrochemical corrosion testing using the Tafel method. For each test, the corrosion parameters, including corrosion potential (Ecorr) and corrosion current (Icorr) were determined (Figure 2). Furthermore, the corroded specimen surface is cleaned with an acetone solution

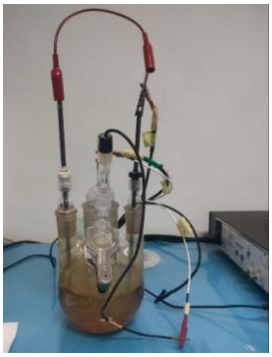

Figure 2. Potentiodynamic polarization (PD) tests

2.3 Materials Characterization

The chemical composition test was carried out using an Optical Emission Spectrometry (ICP-OES ProdigyPlus). Surface of sample observed using a scanning electron microscope (Zeiss Germany EVO MA 10 operated at 20 kV).

3. Results and Discussion

3.1 Corrosion Behavior

The corrosion test results using the resistance polarization method with a 3.5% NaCl solution on Aluminium alloy Al6061 welded with three different types of filler metals (ER4043, ER4047, and ER5356). This test was conducted to obtain the corrosion current (Icorr) values and polarization curves as shown in Figure 3.

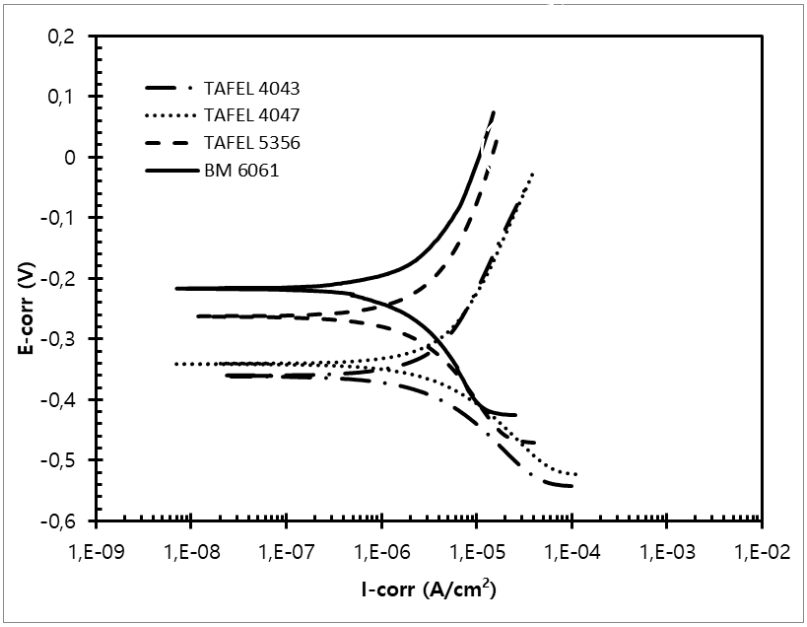

Figure 3. Tafel polarization curves for the base metal and GTAW-welded alloys using ER4043, ER4047, and ER5356 filler metals.

Based on Figure 3, it can be seen that the base metal Al6061 has the lowest Icorr value, which is 0.231 (µA/cm²), and a corrosion potential (Ecorr) of -216.17 mV. Among the three welded joints using different filler metals, the Icorr and Ecorr values are shown in Table 3. It is observed that ER4043 and ER4047 exhibit similar values, while ER5356 shows lower values compared to the other filler metals (-262.867). This result contradicts the findings reported by Ahmed, et al. [9]. They are stated that the lowest corrosion resistance was observed in ER5356 filler metal compared to ER4043.

Table 3. summarizes the corrosion parameters obtained through potentiodynamic polarization testing.

Specimen	E-corr (mV)	I-corr (µA / cm^2)	Corr-rate (mpy)
ER4043	-362.279	0.459	0.202805420
ER4047	-340.989	0.456	0.201479895
ER5356	-262.867	0.324	0.143156767
BM 6061	-216.170	0.231	0.102065473

The differences in Icorr values result in varying corrosion rates in the welded joints of the aluminum alloy, with the joint exhibiting the lowest Icorr value having the best corrosion resistance [9]. According to Table 3, the highest corrosion rate occurred in the welded joint using ER4043 filler, at 0.202805 mpy, while the lowest rate was found in the base metal Al6061, at 0.102065 mpy. The result obtained is lower compared to that reported by [18], which was 1.469 mpy. In the weld zone of all filler variations, the corrosion rate is higher than that of the base material (Al6061). This is due not only to the aggressive environment (3.5% NaCl) but also to the occurrence of galvanic corrosion. Welded joints with dissimilar materials are highly susceptible to galvanic corrosion due to differences in composition (type) between the filler metal and the base material [9].

3.2 SEM observations

Observation of samples using SEM on samples tested for corrosion in 3.5% NaCl media, as shown in Figure 4. The Al6061-T6 base material sample experienced slight deterioration, visible on the sample compared with the welded joints (Figure 4). Figure 4 shows an SEM image of the surface of Aluminum 6061 (Al6061) alloy that has undergone corrosion testing in a 3.5% NaCl solution. The general surface morphology reveals a grain structure that has experienced corrosion attack. A deep and large corrosion pit is visible in the center of the image, indicating significant localized corrosion. Small cracks can be seen around the pit, likely caused by the propagation of damage from within the pit to the surrounding metal structure . The main pit has a large diameter with irregular and rough walls, which are characteristic features of pitting corrosion. Furthermore, small particle fragments or debris are present inside the pit, which corrosion products (such as $Al(OH)_3$ or chloride complex salts). This type of corrosion is often triggered by Cl^- ions in 3.5%NaCl, which can penetrate the natural passive oxide layer on aluminum (Al_2O_3). This form of corrosion is dangerous because it is difficult to detect at an early stage, yet it can lead to sudden material failure.

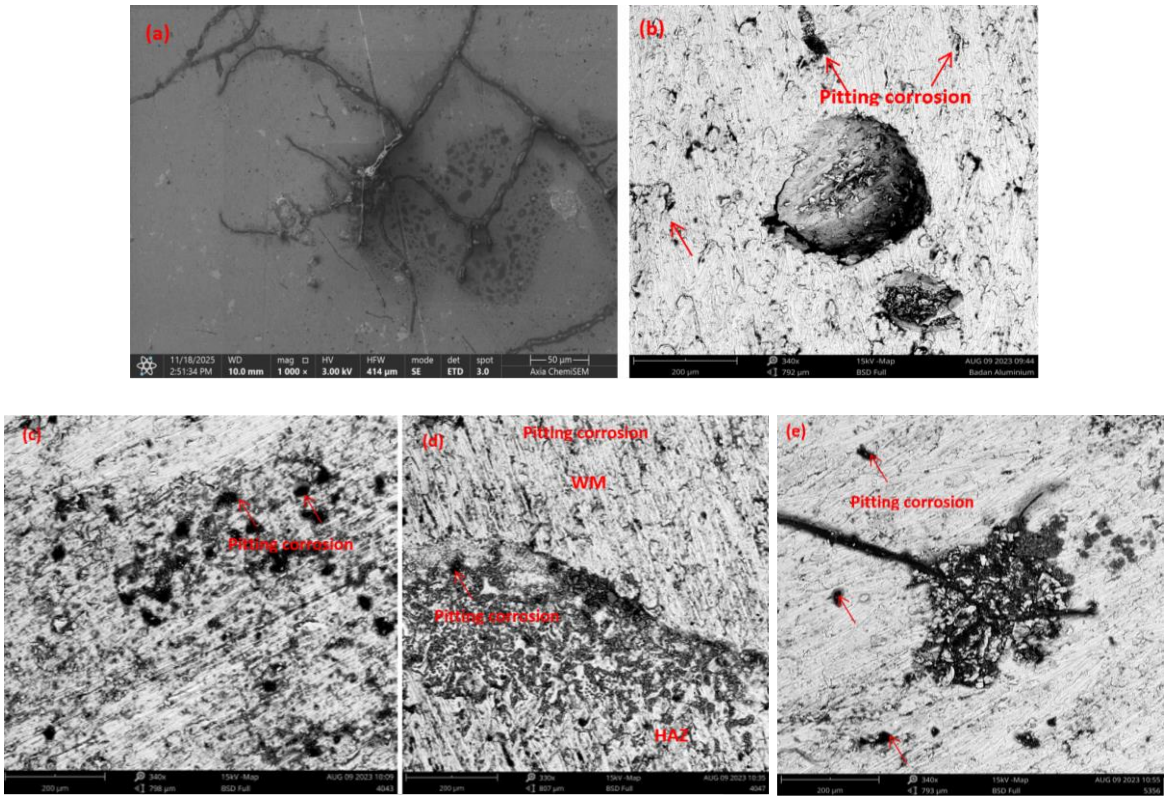

Figure 4. Corrosion surface (a) Al6061 (b) corroded Al6061 surface, c) filler 4043 d) Filler ER4047, e) Filler ER 5356

Surface Morphology Analysis using SEM revealed surface damage on the sample, where distinct pitting corrosion is observed in the form of dark spots of varying sizes, unevenly distributed (Figure 4-c). The distribution of creative corrosion is clearly visible and evenly distributed in the weld metal area of the ER4043 sample (Figure 4-c). This is a typical characteristic of localized corrosion caused by chloride attack on aluminum, particularly in the weld zone containing silicon particles derived from the ER4043 filler. The darker areas are most likely aluminum oxide or other corrosion products, such as $Al(OH)_2Cl_2$ formed due to the reaction with NaCl [19]. The ER4043 contains approximately 5% silicon (Si), which enhances resistance to hot cracking but can also lead to the formation of Al-Si phases that are more susceptible to galvanic corrosion, especially in the presence of potential differences between phases. The main cause is the penetration of Cl^- ions from the NaCl solution through the passive aluminum layer. Furthermore, Pit sizes were found to range from 10 µm (smallest) to 40 µm (largest).

SEM observations revealed two distinct zones: the Heat-Affected Zone (HAZ) and the weld zone. The brighter areas correspond to the HAZ, while the darker, rougher regions represent the weld zone, indicating damage due to corrosion. The boundary line likely marks the transition between the weld zone and the base metal or between the HAZ and the weld zone (Figure 4-d). In the weld zone, pitting corrosion was observed, with pit sizes ranging from small to moderate (estimated at 5–30 µm). The pits appear as dark spots and depressions on the surface, unevenly distributed. A dense pit distribution suggests intensive localized corrosion attack, which is characteristic of pitting corrosion on aluminum in chloride-containing environments. The dark areas likely indicate the presence of corrosion products such as $Al(OH)_3$ or Al_2O_3, formed as a result of the reaction between aluminum and Cl^- ions from NaCl. The presence of fine cracks and rough surface morphology further supports the possibility of corrosion product accumulation. A significant difference can be seen in the sample with filler metal ER4047, wherein the weld area of the creative corrosion appears to be evenly distributed (Figure 4-d).

SEM observations showed that the HAZ (Heat-Affected Zone) is more resistant to corrosion attack compared to the weld metal. These results are in contrast to the findings of Guzmán, et al. [20], who observed uniform and localized corrosion in the Heat-Affected Zone (HAZ) compared to the weld metal in the GMAW welding of Al6061. The ER4047 filler metal contains approximately 12% silicon, significantly higher than ER4043, which contains around 5% silicon (Figure 4-d). This high silicon content improves molten metal flow during welding and reduces the risk of hot cracking. However, it also lead to the formation of brittle Al–Si eutectic phases, which can act as local anodic or cathodic sites, increasing the risk of galvanic corrosion when in contact with pure aluminum phases.

Microstructural analysis using SEM on the weld metal clearly shows evidence of localized corrosion attack, indicated by the presence of dark areas in the central region and several scattered spots. The uneven distribution of dark particles, along with branched crack structures, suggests characteristics of pitting corrosion and underfilm corrosion (Figure 4-e). The very dark areas likely indicate the accumulation of corrosion products such as $Al(OH)_3$ (formed from the reaction between aluminum and chloride ions), and $Mg(OH)_2$ (due to the presence of approximately 5% magnesium in ER5356). The presence of Al_2O_3 is also possible, indicating the breakdown of the passive oxide layer.

The branch-like cracks extending from the corrosion center suggest pit propagation or crack formation associated with stress-assisted corrosion. The presence of large, irregular grains indicate spalling of the passive layer, making the affected area more vulnerable to chloride ion attack. The rough surface morphology surrounding the pits further supports the occurrence of progressive pitting corrosion. The ER5356 filler metal contains magnesium (5%) as a primary alloying element, which enhances mechanical strength but can also form localized anodic regions (Figure 4-e).

The high magnesium content increases the risk of galvanic corrosion when in contact with pure aluminum phases. The observed corrosion also be exacerbated by microstructural heterogeneity resulting from the welding process.

4. Conclusion

This study investigated the corrosion behaviour of Al6061 weld joints produced using the GTAW process with different filler metals (ER4043, ER4047, and ER5356) in a 3.5% NaCl environment. The electrochemical results demonstrate that the welded joints exhibit higher corrosion susceptibility compared to the base metal due to galvanic interactions between heterogeneous weld microstructures. Among the filler variations, the ER5356-welded joint exhibited the lowest corrosion rate, while ER4043 contributed to the highest corrosion rate. SEM characterisation confirmed dominant pitting corrosion in all specimens, with more severe attack observed in the HAZ than in the weld metal area. Overall, ER5356 is recommended as the most suitable filler metal to improve the corrosion performance of Al6061 welded components operating in chloride-rich environments. To further enhance corrosion resistance and strengthen scientific understanding, future studies are suggested to investigate the influence of post-weld heat treatment, investigating ageing treatments to minimise microstructural inhomogeneity and reduce galvanic corrosion effects. Besides, exploring alternative filler wires and hybrid welding, including solid-solution strengthened filler alloys and advanced welding processes to improve joint performance.

Acknowledgement

The author would like to express sincere gratitude to Universitas Muhammadiyah Sumatera Utara for providing financial support for this research under contract number 056/II.3-AU/UMSU-LP2M/C/2023 in the year 2023. The authors would also like to express their sincere appreciation to the Materials Testing Laboratory, Department of Mechanical Engineering, Universitas Gadjah Mada, for kindly granting access and technical support during the corrosion testing activities.

References

[1] K. Uday and G. Rajamurugan, "Influence of tool rotational and transverse speed on friction stir welding of dissimilar aluminum 6061 composites," *Materials Letters*, vol. 329, p. 133182, 2022.

[2] B. Yelamasetti *et al.*, "Synergistic Effects of Optimizing Stir Casting and Friction Stir Welding for WC and Al2O3 based Nano-Particulates Reinforced AA2014 and AA6061 Alloys: Mechanical, Weldability, Corrosion, and Microstructural Morphological Insights," *Journal of Materials Research and Technology*, 2025.

[3] S. Aravind and A. D. Das, "An examination on GTAW samples of 7-series aluminium alloy using response surface methodology," *Materials Today: Proceedings*, vol. 37, pp. 614-620, 2021.

[4] D. Varshney and K. Kumar, "Application and use of different aluminium alloys with respect to workability, strength and welding parameter optimization," *Ain Shams Engineering Journal*, vol. 12, no. 1, pp. 1143-1152, 2021.

[5] H. Mehdi and R. Mishra, "Investigation of mechanical properties and heat transfer of welded joint of AA6061 and AA7075 using TIG+ FSP welding approach," *Journal of Advanced Joining Processes*, vol. 1, p. 100003, 2020.

[6] H. Mehdi and R. Mishra, "Effect of friction stir processing on mechanical properties and heat transfer of TIG welded joint of AA6061 and AA7075," *Defence Technology*, vol. 17, no. 3, pp. 715-727, 2021.

[7] U. Dwivedi, S. Tiwari, A. Mishra, and S. Das, "Comparative study of weld characteristics of Friction stir welded joints on aluminium 7075 with autogenous TIG," *Materials Today: Proceedings,* vol. 22, pp. 2532-2538, 2020.

[8] S. Yan, B. Xing, H. Zhou, Y. Xiao, Q.-H. Qin, and H. Chen, "Effect of filling materials on the microstructure and properties of hybrid laser welded Al-Mg-Si alloys joints," *Materials Characterization,* vol. 144, pp. 205-218, 2018.

[9] M. Ahmed, M. Javidani, A. Maltais, and X.-G. Chen, "Comparison of Mechanical, Fatigue, and Corrosion Properties of Fusion-Welded High-Strength AA6011 Alloy Using Three Filler Wires," *Processes,* vol. 12, no. 6, p. 1172, 2024.

[10] V. Fahimpour, S. Sadrnezhaad, and F. Karimzadeh, "Corrosion behavior of aluminum 6061 alloy joined by friction stir welding and gas tungsten arc welding methods," *Materials & Design,* vol. 39, pp. 329-333, 2012.

[11] D. Priyasudana, S. A. Crisdion, P. Puspitasari, and D. D. Pramono, "Double side friction stir welding effect on mechanical properties and corrosion rate of aluminum alloy AA6061," *Heliyon,* vol. 9, no. 2, 2023.

[12] S. Sinhmar and D. K. Dwivedi, "A study on corrosion behavior of friction stir welded and tungsten inert gas welded AA2014 aluminium alloy," *Corrosion Science,* vol. 133, pp. 25-35, 2018.

[13] Z. Yang and H. Huang, "Corrosion behavior of ADC12 aluminum alloy welded joint using tungsten inert gas welding in 3.5 wt.% NaCl solution," *Materials Chemistry and Physics,* vol. 295, p. 127217, 2023.

[14] P. Li *et al.*, "Effect of post-weld heat treatment on inhomogeneity of mechanical properties and corrosion behavior of rotary friction welded 2024 aluminum alloy joint," *Journal of Manufacturing Processes,* vol. 75, pp. 1012-1022, 2022.

[15] F. Gharavi, K. A. Matori, R. Yunus, N. K. Othman, and F. Fadaeifard, "Corrosion behavior of Al6061 alloy weldment produced by friction stir welding process," *Journal of Materials Research and Technology,* vol. 4, no. 3, pp. 314-322, 2015.

[16] I. A. Soomro, A. Hassan, U. Aftab, L. Zhao, A. Arshad, and B. Shahid, "Investigation of stress corrosion cracking behavior of friction stir welded thick al 6061-t6 alloy plate," *Welding in the World,* pp. 1-11, 2024.

[17] S. Suherman *et al.*, "Analysis of mechanical properties, microstructure, and distortion of Al6061-T6 alloys plate using GTA and GMA welding process," *Jurnal Polimesin,* vol. 23, no. 2, 2025.

[18] I. H. Zainelabdeen, F. A. Al-Badour, A. Y. Adesina, R. Suleiman, and F. A. Ghaith, "Friction stir surface processing of 6061 aluminum alloy for superior corrosion resistance and enhanced microhardness," *International Journal of Lightweight Materials and Manufacture,* vol. 6, no. 1, pp. 129-139, 2023.

[19] Z. Szklarska-Smialowska, "Pitting corrosion of aluminum," *Corrosion science,* vol. 41, no. 9, pp. 1743-1767, 1999.

[20] I. Guzmán *et al.*, "Corrosion Performance and Mechanical Strength in Aluminum 6061 Joints by Pulsed Gas Metal Arc Welding," *Materials,* vol. 15, no. 18, p. 6226, 2022.